View metadata, citation and similar papers at core.ac.uk

brought to you by CORE

provided by NASA Technical Reports Server

N87-22708

SPACE STATION/SHUTTLE ORBITER

DYNAMICS DURING DOCKING

N. G. Fitz-Coy* and J. E. Cochran, Jr.+
Auburn University, AL 36849-3501

Mathematical models of a reference Space Station configuration ("Power Tower") and a Space Shuttle Orbiter are developed and used to study the dynamic behavior of the Space Station/Orbiter system just prior to and subsequent to an impulsive docking of the two spacecraft. The physical model of the Space Station is a collection of rigid and flexible bodies. The orbiter is modeled as a rigid body. An algorhthm developed for use in digitally simulating the dynamics of the system is described and results of its application are presented.

INTRODUCTION

Placing a permanently manned space station in low earth orbit has been identified as the next major goal of the United States civilian space program.[1] This station will serve as a multifunctional base for scientific and commercial advances in space. It will contain laboratories for research in such areas as communication, solar system development, material processing, and astrophysics. The station will also serve as a platform for satellite repair, thus expanding the life span of these expensive space assets and reducing repair costs. In-orbit satellite equipment updating will also be possible, thus assuring that technological developments are quickly incorporated. Additionally, the Space Station will serve as a base for the assembly of other space structures which are too large to be first assembled on earth and then placed into orbit by the Space Shuttle.

The National Aeronautics and Space Administration (NASA) has been assigned the task of defining a reference configuration for the Space Station. From a field of five candidate configurations, NASA has selected the "Power Tower" arrangement (see Fig. 1) as the reference

---

* Graduate Research Assistant.

+ Professor of Aerospace Engineering.

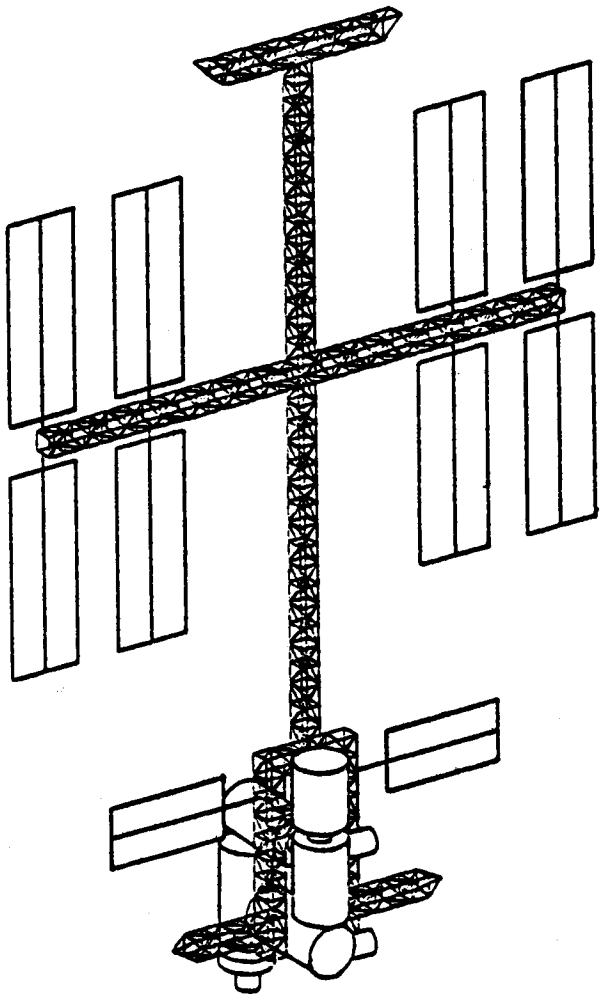

Fig. 1 "Power Tower" Space Station Configuration (Without Payload).

configuration.[2] One of the reasons cited by NASA for selecting the Power Tower configuration is its extraordinary expansion capabilities. This configuration will consist of pressurized modules for habitation and work areas, solar arrays for power acquisition, radiators for heat dispersion, a docking port for the Space Shuttle, and a light-weight truss constructed of carbon epoxy to which all the above are attached. Due to the large size and the expected growth of the Space Station, it is not reasonable to assume that the structure can be analyzed as a rigid body.

The transfer of crew, supplies, and equipment to the Space Station will require frequent docking of a Space Shuttle orbiter with the station. It is therefore important that an understanding of the effects of docking on the motion of the Space Station/Space Shuttle system be developed. Estimates of these effects on the motion of the proposed Space Station configuration are needed to adequately design its attitude and translational control systems. Careful investigation of the docking process should result in improvements in the reference configuration.

It is expected that the closing rate of an orbiter with the Space Station will be small (on the order of 1.0 ft/sec). However, due to the high degree of flexibility of the station, the docking of the orbiter may still produce significant deflections of parts of the station. The rare possibility of a Space Station control systems malfunction requires that docking of the orbiter with an uncontrolled Space Station be considered. Furthermore, the dynamic response of an uncontrolled Space Station/Orbiter system during docking is of considerable importance from the standpoint of control system design.

Early studies on docking involved investigators such as Williams,[3] Grubin,[4] Chiarappa,[5] Brayton,[6] and Cochran and Henderson.[7] With the exception of the work done by Cochran and Henderson, these early studies were not concerned with the effects of flexibility on docking. In considering the effects of flexibility, Cochran and Henderson analyzed a system consisting of a rigid target vehicle to which two point masses are connected by massless, flexible, extensible rods. A rigid rendezvous vehicle was allowed to dock with the target vehicle and the effects of the flexibility of the appendages were then analyzed.

Recently, the problem of spacecraft flexibility has received renewed attention. In particular, Levinson and Kane,[8,9,10] have considered the planar docking dynamics of bodies consisting of flexible and rigid components. Some of the work done by Levinson and Kane involves the docking dynamics of (1) a spacecraft modeled as a cantilever beam and a rigid rendezvous vehicle, and (2) a spacecraft modeled as a free-free beam and a rigid rendezvous vehicle.[9,10] In these analyses, the deformation of the structure was represented by unconstrained mode shapes which were obtained using a finite element approach. It was shown by Hablani[11] that unconstrained mode shapes portray the deformation of the structure more accurately than constrained mode shapes. Here, "constrained mode shapes" refers to mode shapes obtained when one end of the structure is constrained and the

structure is then caused to vibrate at its natural frequencies. On the other hand, unconstrained mode shapes are obtained when the structure is completely free. Many other investigators such as Likins,[12] Hughes and Skelton[13] and Ho and Herber[14] have developed simulation routines and modal truncation methods to analyze the effects of flexibility on large spacecraft.

The docking problem considered in this paper differs from the work done by Levinson and Kane. Herein, the motion is three-dimensional rather than planar and a more complex model of one of the bodies is developed and utilized. Unconstrained mode shapes are used to define the motion of the structure. These mode shapes were obtained from the MacNeal-Schwendler (MSC) Nastran[16] finite-element modal analysis routine. They were incorporated in a computer program developed to simulate the dynamics of the Space Station before and after docking. A particular docking mechanism is not considered; instead, the docking is modeled as an impulsive interaction between the Space Station and an Orbiter.

In the following sections the governing equations of the Space Station/Orbiter system are derived and simulation results are presented. The motions of the Space Station and Space Station plus Orbiter system are considered first. Next, the equations governing the impulsive interaction between the Station and an Orbiter are derived. Use of the complete set of equations to simulate the motion of the Space Station before and after docking with an Orbiter occurs is then discussed. Representative simulation results are presented and interpreted. Finally, conclusions are stated along with suggestions for additional research.

EQUATIONS OF MOTION

The station is modeled as a hybrid of flexible and rigid components in which the base section (lower section containing the modules and the docking port) is modeled as a system of rigid bodies and the remaining structure (upper and lower keels, booms, and solar arrays) is modeled as a collection of flexible bodies. The center of mass of the undeformed station is assumed to move in a circular orbit about the earth. Because impulsive docking is assumed, the presence in the system of the Orbiter after docking is modeled by adding a rigid body to the base section of the original Station model.

As shown in Fig. 2, the inertial position vector $\underline{R}_p$ of a generic mass element, P, of mass, dm, can be written as

$$\underline{R}_p = \underline{R}_s + \underline{r} \ , \tag{1}$$

where $\underline{r}$ includes vectors for both the deformed and undeformed structure. If the structure is assumed to be flexible, the vector $\underline{r}$ can be expressed as

$$\underline{r} = \underline{r}_u + \underline{u} \ . \tag{2}$$

As shown in Fig. 3, $\underline{r}_u$ is the vector locating the point P in the $SX_sY_sZ_s$ system when the structure is undeformed; and $\underline{u}$ defines the deformation of the structure in the $SX_sY_sZ_s$ system. The $SX_sY_sZ_s$ system is tied to the station in such a way that S coincides with the station's mass center when the structure is undeformed. The nominal orientation of this coordinate system is such that the X_s-axis is tangent to the orbit, the Y_s-axis is parallel to the boom and points towards starboard, and the Z_s-axis is parallel to the keel and is directed radially towards the center of the earth. When docking occurs, the $SX_sY_sZ_s$ system rotates with the Space Station. If the deformation is defined in terms of unconstrained mode shape vectors, $\underline{\phi}_k$, then $\underline{u}$ can be written as

$$\underline{u} = \sum_{k=1}^{N} \underline{\phi}_k q_k, \tag{3}$$

where $\underline{\phi}_k$ is the mode shape of the k^{th} mode, and q_k is the generalized coordinate associated with the k^{th} mode. Substitution of Eq. (2) into Eq. (1) results in

$$\underline{R}_p = \underline{R}_s + \underline{r}_u + \underline{u}. \tag{4}$$

The translational equations of motion are obtained from

$$\int_{M_s} \underline{f} dm = \int_{M_s} \underline{a}_p dm = \int_{M_s} \ddot{\underline{R}}_p dm, \tag{5}$$

where $\underline{f}$ is the force per unit mass acting on the differential element of mass, dm, and M_s is the total station mass.

From Eq. (4), $\ddot{\underline{R}}_p$ can be expressed as

$$\ddot{\underline{R}}_p = \ddot{\underline{R}}_s + \dot{\underline{\omega}}_s \times (\underline{r}_u + \underline{u}) + \underline{\omega}_s \times [\underline{\omega}_s \times (\underline{r}_u + \underline{u})] + 2\underline{\omega}_s \times \dot{\underline{u}} + \ddot{\underline{u}} \ , \tag{6}$$

where $\underline{\omega}_s$ is the angular velocity of the $SX_sY_sZ_s$ system and a "$\cdot$" over a vector denotes time differentiation of that vector's X_s-, Y_s- and Z_s-components only. Substituting Eqs. (3) and (6) into Eq. (5), the resulting equation can be evaluated to obtain the following matrix form of the translational equations of motion:

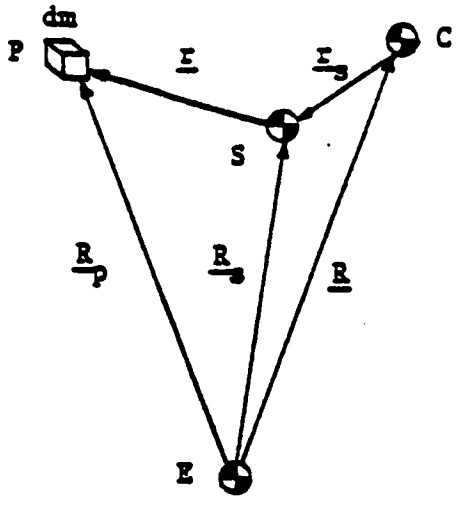

Fig. 2. Inertial Position Vector of Differential Element, dm.

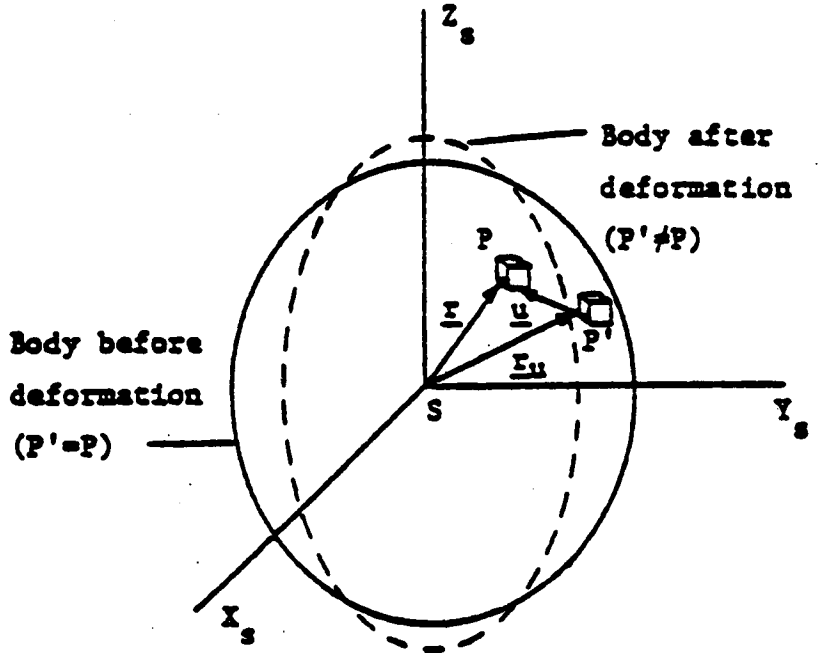

Fig. 3. Description of Space Station's Deformation in the $SX_sY_sZ_s$ System.

$$\underline{F}^{ex} = M_s \ddot{\underline{R}}_s + \underline{\underline{C}}^T \sum_{k=1}^{N} [(\dot{\tilde{\underline{\omega}}}_s + \tilde{\underline{\omega}}_s \tilde{\underline{\omega}}_s) \underline{m}_k q_k$$

$$+ 2\tilde{\underline{\omega}}_s \underline{m}_k \dot{q}_k + \underline{m}_k \ddot{q}_k] \tag{7}$$

where $\underline{m}_k$ is the modal momentum coefficient[11] defined as

$$\underline{m}_k = \int_{M_s} \underline{\phi}_k \, dm \, , \tag{8}$$

and $\underline{F}^{ex}$ is the total external force. The direction cosine matrix, $\underline{\underline{C}}^T$, is also introduced to accommodate the different coordinate systems used in writing Eq. (6). Here, $\underline{\underline{C}}^T$ transforms vector components in $SX_sY_sZ_s$ system to corresponding components in the EXYZ system. Thus, Eq. (7) represents the translational equations of motion written in the EXYZ system.

The rotational equations of motion about the station's mass center are obtained from

$$\int_{M_s} \underline{\tau} \, dm = \int_{M_s} \underline{r} \times \underline{a}_p dm, \tag{9}$$

where $\underline{\tau}$ is the torque per unit mass about S due to the force per unit mass $\underline{f}$. The left side of Eq. (12) is the total external torque about the station's mass center; that is,

$$\int_{M_s} \underline{\tau} \, dm = \underline{T}^{ex} \, . \tag{10}$$

By substituting Eqs. (2), (6), and (10) into Eq. (9), and evaluating the integrals which appear in the resulting equation, one may rewrite Eq. (9) in the matrix form,

$$T^{ex} = \sum_{k=1}^{N} [q_k \tilde{\underline{m}}_k \underline{\underline{C}} \ddot{\underline{R}}_s + \underline{\underline{I}} \dot{\underline{\omega}}_s + \tilde{\underline{\omega}}_s \underline{\underline{I}} \underline{\omega}_s$$

$$+ 2\underline{\underline{A}}_k \underline{\phi}_k q_k + 2\underline{\underline{D}}_k \underline{\phi}_k \dot{q}_k + (\underline{\mu}_k + \sum_{j=1}^{N} \underline{\beta}_{kj} q_j) \ddot{q}_k] \, , \tag{11}$$

where $\underline{\underline{I}}$ is the inertia dyadic of the station. The flexibility coefficient,[11] $\underline{\mu}_k$, of Eq. (11) is defined as

$$\underline{\mu}_k \triangleq \int_{M_s} \tilde{\underline{r}}_u \underline{\phi}_k \, dm \tag{12}$$

and

$$\underline{\beta}_{kj} \triangleq \int_{M_s} \tilde{\underline{\phi}}_j \underline{\phi}_k \, dm \ .$$

Again, the direction cosine matrix, $\underline{\underline{C}}$, has been used to transform the components of vectors to a common reference coordinate system (i.e., the $SX_sY_sZ_s$ system in this case).

Equations (7) and (11) constitute six of the six plus N (6+N) equations needed to define the motion. The remaining N equations are obtained from the equations

$$\int_{M_s} \underline{\phi}_j \cdot \underline{f} \, dm = \int_{M_s} \underline{\phi}_j \cdot \underline{a}_p \, dm \quad , \ j=1,2,\ldots,N, \tag{13}$$

where $\underline{a}_p$ is given by Eq. (6). Generalized forces, Q_j, $j=1,2,3,\ldots,N$, may be defined by

$$Q_j = \int_{M_s} \underline{\phi}_j \cdot \underline{f} \, dm = \int_{M_s} \underline{\phi}_j \cdot \underline{f}^{ex} dm + \int_{M_s} \underline{\phi}_j \cdot \underline{f}^{in} dm \ , \tag{14}$$

where $\underline{f}^{ex}$ and $\underline{f}^{in}$ are the "external" and "internal" parts of $\underline{f}$. Thus, Eq. (13) can be rewritten as

$$Q_j = \int_{M_s} [\underline{\phi}_j \cdot \ddot{\underline{R}}_s + \underline{\phi}_j \cdot \dot{\underline{\omega}}_s \times (\underline{r}_u + \underline{u}) + \underline{\phi}_j \cdot \underline{\omega}_s \times \{\underline{\omega}_s \times (\underline{r}_u + \underline{u})\}$$

$$+ 2\underline{\phi}_j \cdot \underline{\omega}_s \times \dot{\underline{u}} + \underline{\phi}_j \cdot \ddot{\underline{u}}] dm \ . \tag{15}$$

The integrals on the right-hand side of Eq. (15) may be evaluated to obtain the following matrix form for Eq. (15):

$$Q_j = \underline{m}_j^T \underline{\underline{C}} \ddot{\underline{R}}_s + (\underline{\mu}_k^T + \sum_{j=1}^{N} \underline{\beta}_{kj}^T q_j)\dot{\underline{\omega}}_s + \underline{\omega}_s^T \underline{\underline{R}}_j \underline{\omega}_s$$

$$+ \sum_{k=1}^{N} \underline{\omega}_s^T \underline{\underline{P}}_{jk} \underline{\omega}_s q_k + 2 \sum_{k=1}^{N} \underline{\omega}_s^T \underline{\beta}_{jk} \dot{q}_k + \sum_{k=1}^{N} m_{jk} \ddot{q}_k, \tag{16}$$

where

$$\underline{\underline{R}}_j \triangleq \int_{M_s} \tilde{\underline{\phi}}_j \tilde{\underline{r}}_u \, dm \, , \tag{17a}$$

$$\underline{\underline{P}}_{jk} \triangleq \int_{M_s} \tilde{\underline{\phi}}_j \tilde{\underline{\phi}}_k \, dm \, , \tag{17b}$$

$$m_{jk} \triangleq \int_{M_s} \underline{\phi}_j^T \underline{\phi}_k \, dm \, . \tag{17c}$$

Since the elastic deformations are assumed small (i.e., less than 10% of the structural length), then all terms second-order and higher-order in q_k are dropped from Eqs. (7), (11), and (16). Similar action is taken regarding the angular velocity, $\underline{\omega}_s$, of the station. Also, all products of q_k and $\underline{\omega}_s$ are neglected.

By dropping the appropriate terms from Eqs. (7), (11), and (16), one may rewrite these equations as follows:

$$\underline{F}^{ex} = M_s \ddot{\underline{R}}_s + \underline{\underline{C}}^T \sum_{k=1}^{N} [- \tilde{\underline{m}}_k q_k \dot{\underline{\omega}}_s + \underline{m}_k \ddot{q}_k], \tag{18}$$

$$\underline{T}^{ex} = \sum_{k=1}^{N} [q_k \tilde{\underline{m}}_k \underline{\underline{C}} \ddot{\underline{R}}_s + \underline{\underline{I}} \dot{\underline{\omega}}_s + \underline{\mu}_k \ddot{q}_k], \tag{19}$$

$$Q_j = \underline{m}_j^T \underline{\underline{C}} \ddot{\underline{R}}_s + \underline{\mu}_k^T \dot{\underline{\omega}}_s + \sum_{k=1}^{N} m_{jk} \ddot{q}_k \, . \tag{20}$$

Explicit expressions for the forces and torques expressed in Eqs. (18), (19), and (20) are now developed.

Forces and Torques

A satellite in a low earth orbit (nominally 300 km altitude) is affected by several forces. For example, the important external forces and torques may include those due to gravity, the atmosphere, thrusters, other control devices, and solar radiation. In this paper, gravitational forces and gravity-gradient torques are the only external forces and torques considered.

The gravitational force acting on a differential element of mass, dm, is expressed as

$$\underline{f}^g = -\frac{\mu_o}{R_p^3}\underline{R}_p \ , \tag{21}$$

where μ_o is the gravitational constant of the earth and $\underline{R}_p$ is the vector shown in Fig. 4.

By recalling Eq. (1), one can approximate R_p^{-3} by (Ref. 17)

$$R_p^{-3} = \frac{1}{R_s^3}\left[1 - \frac{3}{R_s^2}\underline{r} \cdot \underline{R}_s + \text{H.O.T.}\right] \tag{22}$$

By substituting Eqs. (1) and (22) into Eq. (21), and then integrating, one may show that

$$\begin{aligned}\underline{F}^{ex} = \underline{F}^g = &-\frac{\mu_o}{R_s^3}M_s\underline{R}_s - \frac{\mu_o}{R_s^3}\underline{\underline{C}}^T\sum_{k=1}^{N}\underline{m}_k q_k \\ &+ \frac{3\mu_o}{R_s^5}\sum_{k=1}^{N}(q_k\underline{\underline{C}}^T\underline{m}_k\underline{R}_s)\underline{R}_s \\ &+ \frac{3}{2}\frac{\mu_o}{R_s^5}\underline{\underline{C}}^T t_r(\underline{\underline{I}})\underline{R}_s - 3\frac{\mu}{R_s^5}\underline{R}_s\underline{\underline{C}}^T\underline{\underline{I}} + \text{H.O.T.}\end{aligned} \tag{23}$$

Next, the contribution by terms containing R_s^{-5} may be neglected and the external force expressed (in the EXYZ system) as

$$\underline{F}^{ex} = -\frac{\mu_o}{R_s^3}\left[M_s\underline{R}_s + \underline{\underline{C}}^T\sum_{k=1}^{N}\underline{m}_k q_k\right] . \tag{24}$$

It was noted by Kaplan[18] that gravity-gradient torques provide excellent directional stability for spacecraft in eccentric orbits. Thus, in considering a circular orbit (eccentricity equals zero), it is reasonable to assume that gravity-gradient torques may be used to provide stabilization for the Space Station. The gravity-gradient torque can be obtained by crossing the vector $\underline{r}$ with the external forces defined in Eq. (21) (Ref. 17, pp. 112-119) and is presented here as

$$\underline{T}^{ex} = \frac{\mu_o}{R_s^3}\left[\underline{\underline{\tilde{C}}}\underline{R}_s\sum_{k=1}^{N}\underline{m}_k q_k + \frac{3}{R_s^2}\underline{\underline{\tilde{C}}}\underline{R}_s\underline{\underline{I}}\underline{\underline{C}}\underline{R}_s\right]. \tag{25}$$

Equation (25) represents a set of differential equations, written in the $SX_sY_sZ_s$ system, that governs the rotational motion of the Space Station.

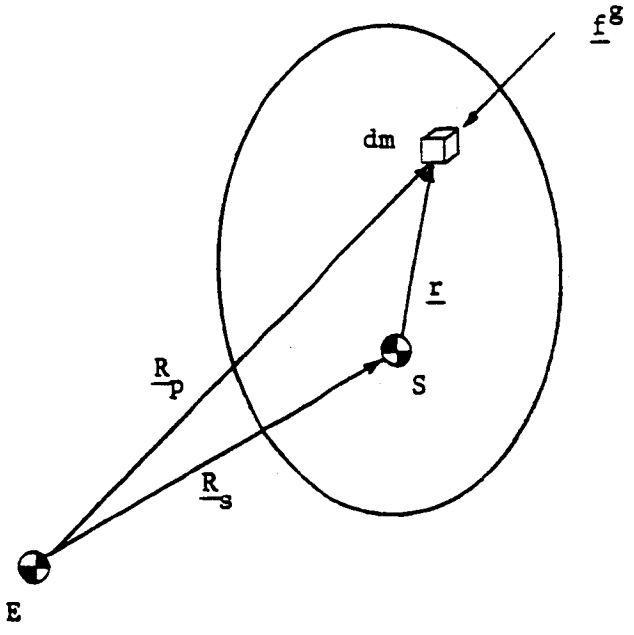

Fig. 4 Gravitational Force Acting on dm.

The generalized force, Q_j, associated with the j^{th} mode of vibration can be decomposed into two parts. One part contains the contribution due to internal forces, and the other contains the contribution due to external forces. Each contribution can be formulated as shown in the following set of equations.

$$Q_j = Q_j^{in} + Q_j^{ex} \tag{26a}$$

$$Q_j^{in} = \sum_{k=1}^{N} m_{jk}\ddot{q}_k + \sum_{k=1}^{N} c_{jk}\dot{q}_k + \sum_{k=1}^{N} k_{jk}q_k \tag{26b}$$

$$Q_j^{ex} = -\frac{\mu_o}{R_s^3}\left[\underline{R}_s^T \underline{\underline{C}}^T \underline{m}_j + \gamma_j + \sum_{k=1}^{N} m_{jk}q_k\right] \tag{26c}$$

In Eqs. (26), c_{jk} and k_{jk} represent the jk^{th} element of the structural damping and stiffness matrices. The quantity γ_j in Eq. (26) is defined as follows:

$$\gamma_j \triangleq \int_{M_s} \underline{\phi}_j^T (\underline{r}_u)dm. \tag{27}$$

The complete linearized equations of motion are obtained by combining Eqs. (18), (19), and (20) with Eqs. (24), (25), and (26). From these expressions, one may show that the equations that govern the translation motion may be expressed as

$$-\frac{\mu_o}{R_s^3}\left[M_s\underline{R}_s + \underline{\underline{C}}^T \sum_{k=1}^{N} \underline{m}_k q_k\right]$$

$$= M_s\ddot{\underline{R}}_s + \underline{\underline{C}}^T \sum_{k=1}^{N} \left[-\tilde{\underline{m}}_k q_k \dot{\underline{\omega}}_s + \underline{m}_k \ddot{q}_k\right], \tag{28}$$

whereas, the rotational motion is governed by

$$\frac{\mu_o}{R_s^3}\left[\tilde{\underline{\underline{C}}}\underline{R}_s \sum_{k=1}^{N} \underline{m}_k q_k + \frac{3}{R_s^2}\,\tilde{\underline{\underline{C}}}\underline{R}_s \underline{\underline{I}}\underline{\underline{C}}\underline{R}_s\right]$$

$$= \sum_{k=1}^{N} \left[q_k \tilde{\underline{m}}_k \underline{\underline{C}}\ddot{\underline{R}}_s + \underline{\underline{I}}\dot{\underline{\omega}}_s + \underline{\mu}_k \ddot{q}_k\right]. \tag{29}$$

The generalized coordinates are governed by the following expression:

$$-\frac{\mu_o}{R_s^3}\left[\sum_{k=1}^{N} m_{jk}q_k + \underline{R}_s^T \underline{\underline{C}}^T \underline{m}_j + \gamma_j\right] + \sum_{k=1}^{N} m_{jk}\ddot{q}_k + \sum_{k=1}^{N} c_{jk}\dot{q}_k + \sum_{k=1}^{N} k_{jk}q_k$$

$$= \underline{m}_j^T \underline{\underline{C}} \ddot{\underline{R}}_s + \underline{\mu}_j^T \dot{\underline{\omega}}_s + \sum_{k=1}^{N} m_{jk}\ddot{q}_k \quad . \tag{30}$$

The 6+N linearized differential equations expressed in Eqs. (28), (29), and (30) are sufficient to simulate the motion of the station before and after docking. To simulate motion after docking, M_s and $\underline{\underline{I}}$ must be adjusted to account for the presence of the orbiter that is now attached to the station.

DOCKING

As stated previously, a particular docking mechanism is not considered in this paper. Instead, the docking of the orbiter with the Space Station is assumed to produce impulsive changes in the kinematical variables. In what follows, the docking of the orbiter with the Space Station is modeled as rigid body docking with a cantilever beam/rigid body assembly. A similar problem was addressed by Levinson and Kane in Ref. 10 where they analyzed the planar case of a rigid body docking with a free beam.

The system to be analyzed (see Fig. 5) consists of a single rigid body (orbiter) and a cantilever beam/rigid body assembly (Station). The system of Fig. 5 can be subdivided into the systems of Fig. 6.

The Space Station (bodies A and B) is assumed to have linear and angular velocities, $\underline{u}_s$ and $\underline{\omega}_s$, before docking occurs. After docking, these velocities become $\underline{v}_s$ and $\underline{\Omega}_s$, respectively. The orbiter's linear velocity will change from $\underline{u}_o$ to $\underline{v}_o$ due to docking. Also, the angular velocity of the orbiter will change from $\underline{\omega}_o$ to $\underline{\Omega}_s$. As stated above, the orbiter and the Space Station are assumed to couple rigidly during docking, and then to rotate together.

Equations for Docking

The law of conservation of linear momentum for body A can be expressed as

$$\int_{m_A} (\underline{v}_a - \underline{u}_a)dm = \int_{t_1}^{t_2} (\int \underline{f}\, dm)dt \quad , \tag{31}$$

where m_A is the mass of body A. The quantities $\underline{u}_a$ and $\underline{v}_a$ are the "before" and "after" velocities of a differential element of mass, dm, and are defined here as

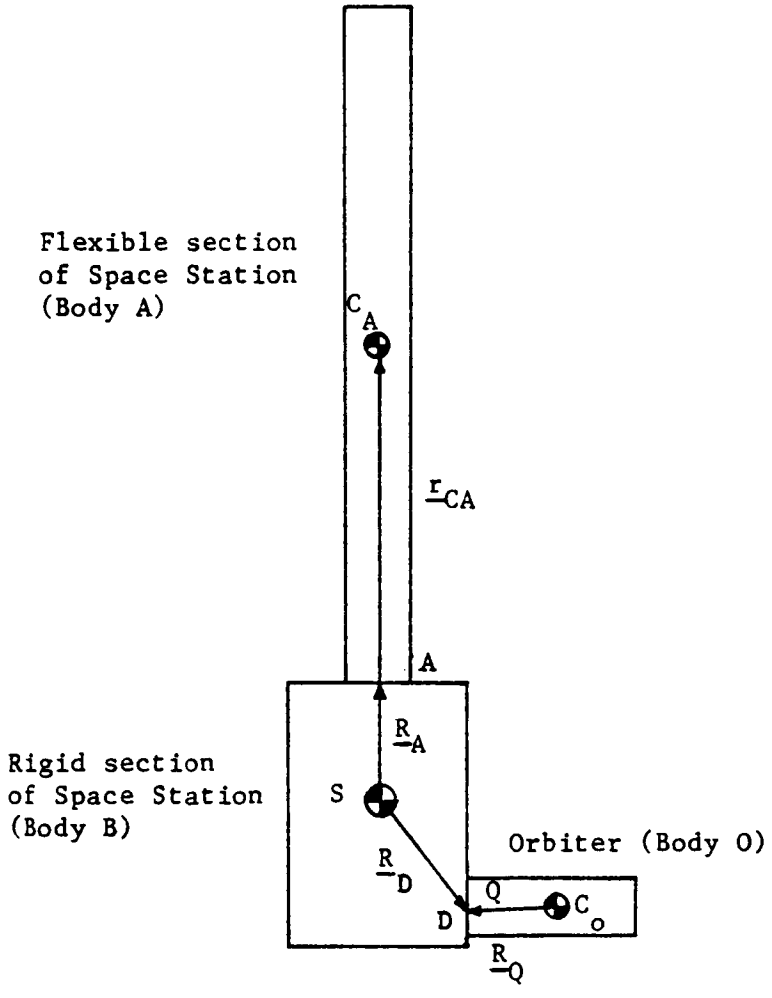

Fig. 5. Schematic of Orbiter/Space Station Assembly.

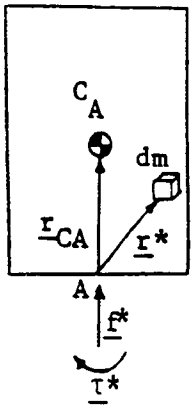

Fig. 6(a). Free-Body Diagram for Flexible Section of the Space Station (Body A).

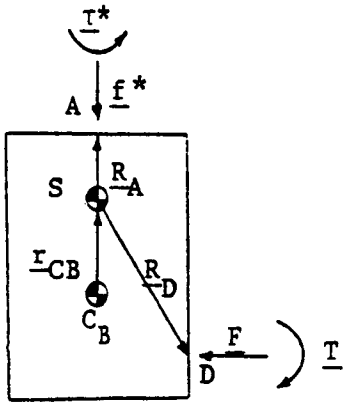

Fig. 6(b). Free-Body Diagram for Rigid Section of the Space Station (Body B).

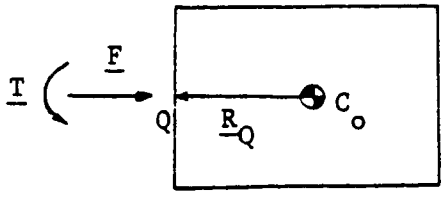

Fig. 6(c). Free-Body Diagram for the Orbiter (Body O).

$$\underline{u}_a = \underline{u}_s + \underline{\omega}_s \times \underline{R}_A + \underline{\omega}_s \times \underline{r}^* + \sum_{k=1}^{N} \underline{\phi}_k \dot{q}_k^- \tag{32a}$$

and

$$\underline{v}_a = \underline{v}_s + \underline{\Omega}_s \times \underline{R}_A + \underline{\Omega}_s \times \underline{r}^* + \sum_{k=1}^{N} \underline{\phi}_k \dot{q}_k^+ \tag{32b}$$

where $\dot{q}_k^-$ and $\dot{q}_k^+$ are the "before" and "after" time rate of change of the generalized coordinates. Equation (32) may be substituted into Eq. (31), and the result integrated to obtain the following form of the statement of the law of conservation of linear momentum for body A:

$$m_A (\underline{v}_s - \underline{u}_s) + m_A (\underline{\Omega}_s - \underline{\omega}_s) \times (\underline{R}_A + \underline{r}_{CA}) + \sum_{k=1}^{N} \underline{P}_k (\dot{q}_k^+ - \dot{q}_k^-)$$

$$= - \int_{t_1}^{t_2} \underline{f}^* \, dt \, . \tag{33}$$

The quantity $\underline{P}_k$ shown in Eq. (33) represents the momentum flexibility coefficient[11] for body A and is defined as

$$\underline{P}_k \triangleq \int_{m_A} \underline{\phi}_k \, dm \, .$$

The law of conservation of linear momentum may also be applied to bodies B and O. For body B, one has

$$m_B (\underline{v}_s - \underline{u}_s) = \int_{t_1}^{t_2} (\underline{F} + \underline{f}^*) dt, \tag{34}$$

and for body O,

$$m_o (\underline{v}_o - \underline{u}_o) = - \int_{t_1}^{t_2} \underline{F} \, dt \tag{35}$$

Equations (33), (34), and (35) may be combined to give

$$m_A (\underline{v}_s - \underline{u}_s) + m_A (\underline{\Omega}_s - \underline{\omega}_s) \times (\underline{R}_A + \underline{r}_{CA}) + \sum_{k=1}^{N} \underline{P}_k (\dot{q}_k^+ - \dot{q}_k^-)$$

$$+ m_B (\underline{v}_s - \underline{u}_s) + m_o (\underline{v}_o - \underline{u}_o) = \underline{0} \tag{36}$$

The dot product of $\underline{\phi}_j$ with Eqs. (31) and (32) combined provides an expression for $\dot{q}_k^+ - \dot{q}_k^-$.

$$\int_m [(\underline{v}_s - \underline{u}_s) \cdot \underline{\phi}_j + (\underline{\Omega}_s - \underline{\omega}_s) \times (\underline{R}_A + \underline{r}^*) \cdot \underline{\phi}_j$$

$$+ \sum_{k=1}^{N} \underline{\phi}_j \cdot \underline{\phi}_k (\dot{q}_k^+ - \dot{q}_k^-)] \, dm = - \int_{t_1}^{t_2} \underline{\phi}_j \cdot \underline{f}^* \, dt \qquad (37)$$

The right-hand side of Eq. (37) is zero because at the point at which $\underline{f}^*$ is applied, the deformation is zero. Thus, Eq. (37) can be rewritten in matrix form as

$$\underline{P}_j^T(\underline{v}_s - \underline{u}_s) - \underline{P}_j^T \tilde{\underline{R}}_A(\underline{\Omega}_s - \underline{\omega}_s) + \underline{G}_j^T(\underline{\Omega}_s - \underline{\omega}_s)$$

$$= - \sum_{k=1}^{N} m_{jk}(\dot{q}_k^+ - \dot{q}_k^-) \qquad (38)$$

where

$$\underline{G}_j = \int_{m_A} \tilde{\underline{r}}^* \underline{\phi}_j \qquad (39a)$$

and

$$m_{jk} = \int_{m_A} \underline{\phi}_j^T \underline{\phi}_k \, dm \, . \qquad (39b)$$

To account for the N modes of vibration, Eq. (38) can be rewritten in the following form:

$$\underline{\underline{P}}^T(\underline{v}_s - \underline{u}_s) - \underline{\underline{P}}^T \tilde{\underline{R}}_A(\underline{\Omega}_s - \underline{\omega}_s) + \underline{\underline{G}}^T(\underline{\Omega}_s - \underline{\omega}_s) = \underline{\underline{M}}\dot{\underline{q}} \, , \qquad (40)$$

The Nx3 matrices, $\underline{\underline{P}}^T$ and $\underline{\underline{G}}^T$, are defined as:

$$\underline{\underline{P}}^T = \begin{bmatrix} \underline{P}_1^T \\ \underline{P}_2^T \\ \vdots \\ \underline{P}_N^T \end{bmatrix} , \quad \underline{\underline{G}}^T = \begin{bmatrix} \underline{G}_1^T \\ \underline{G}_2^T \\ \vdots \\ \underline{G}_N^T \end{bmatrix} . \qquad (41a)$$

$$\underline{\underline{M}} = -\begin{bmatrix} m_{11} & m_{12} & \cdots & m_{1N} \\ m_{21} & & & \\ \vdots & & & \\ m_{N1} & \cdots & & m_{NN} \end{bmatrix} \quad ; \quad \dot{\underline{q}} = \begin{bmatrix} \dot{q}_1^+ - \dot{q}_1^- \\ \dot{q}_2^+ - \dot{q}_2^- \\ \vdots \\ \dot{q}_N^+ - \dot{q}_N^- \end{bmatrix} \tag{41b}$$

The law of conservation of angular momentum yields three additional expressions. These expressions are obtained from the following equations by applying the law of conservation of angular momentum to bodies A and B combined (Space Station), and to body O (Orbiter). Equation (42) is obtained when the law of conservation is applied to the Space Station.

$$(\underline{\underline{I}}_s + \underline{\underline{I}}_A^*) \cdot (\underline{\Omega}_s - \underline{\omega}_s) + [m_A(\underline{R}_A + \underline{r}_{CA}) + \sum_{k=1}^{N} \underline{P}_k q_k] \times (\underline{v}_s - \underline{u}_s)$$

$$+ \underline{R}_A \times \sum_{k=1}^{N} \underline{P}_k \dot{q}_k + \sum_{k=1}^{N} \underline{G}_k \dot{q}_k = \int_{t_1}^{t_2} [\underline{T} + \underline{R}_D \times \underline{F}] dt \tag{42}$$

A similar expression is obtained for body O (Orbiter).

$$\underline{\underline{I}}_o \cdot (\underline{\Omega}_s - \underline{\omega}_s) = -\int_{t_1}^{t_2} [\underline{T} + \underline{R}_Q \times \underline{F}] \, dt \tag{43}$$

If one combines Eqs. (35), (42) and (43), then the statement of conservation of angular momentum can be expressed in the following matrix form:

$$(\underline{\underline{I}}_s + \underline{\underline{I}}_A^* + \underline{\underline{I}}_D) \, \underline{\Omega}_s + [m_A(\tilde{\underline{R}}_A + \tilde{\underline{r}}_{CA}) + \underline{\underline{P}}\underline{q}](\underline{v}_s - \underline{u}_s) + [\tilde{\underline{R}}_A \underline{\underline{P}} + \underline{\underline{G}}] \, \dot{\underline{q}}$$

$$+ m_o(\tilde{\underline{R}}_D - \tilde{\underline{R}}_Q)(\underline{v}_o - \underline{u}_o) = (\underline{\underline{I}}_s + \underline{\underline{I}}_A^*) \, \underline{\omega}_s + \underline{\underline{I}}_o \, \underline{\omega}_o \tag{44}$$

Equations (36), (40), and (44) represent six plus N (6+N) equations in nine plus N (9+N) unknowns. The relationship between $\underline{v}_s$ and $\underline{v}_o$ accounts for the remaining three equations. This relationship is written here as

$$\underline{v}_o = \underline{v}_s - (\tilde{\underline{R}}_D - \tilde{\underline{R}}_Q) \, \underline{\Omega}_s . \tag{45}$$

It can be shown that Eqs. (36), (40), (44), and (45), when combined, yield the following equations that govern the impulsive interaction between the Station and the Orbiter.

$$[\underline{\underline{P}}\underline{\underline{M}}^{-1}(\underline{\underline{G}}^T - \underline{\underline{P}}^T\tilde{\underline{R}}_A) - m_A(\tilde{\underline{R}}_A + \tilde{\underline{r}}_{CA}) - m_o(\tilde{\underline{R}}_D - \tilde{\underline{R}}_Q)]\,\underline{\Omega}_s$$

$$+ [(m_A + m_B + m_o)\,\underline{\underline{E}} + \underline{\underline{P}}\underline{\underline{M}}^{-1}\underline{\underline{P}}^T]\,\underline{v}_s$$

$$= [(m_A + m_B)\,\underline{\underline{E}} + \underline{\underline{P}}\underline{\underline{M}}^{-1}\underline{\underline{P}}^T]\,\underline{u}_s + m_o\,\underline{u}_o$$

$$+ [\underline{\underline{P}}\underline{\underline{M}}^{-1}(\underline{\underline{G}}^T - \underline{\underline{P}}^T\tilde{\underline{R}}_A) - m_A(\tilde{\underline{R}}_A + \tilde{\underline{r}}_{CA})]\,\underline{\omega}_s \qquad (46)$$

$$[\underline{\underline{I}}_s + \underline{\underline{I}}^*_A + \underline{\underline{I}}_o - m_o(\tilde{\underline{R}}_D - \tilde{\underline{R}}_Q)(\tilde{\underline{R}}_D - \tilde{\underline{R}}_Q)$$

$$+ (\tilde{\underline{R}}_A\underline{\underline{P}} + \underline{\underline{G}})\,\underline{\underline{M}}^{-1}(\underline{\underline{G}}^T - \underline{\underline{P}}^T\tilde{\underline{R}}_A)]\,\underline{\Omega}_s$$

$$+ [m_A(\tilde{\underline{R}}_A + \tilde{\underline{r}}_{CA}) + \tilde{\underline{\underline{P}}}\underline{q} + m_o(\tilde{\underline{R}}_D - \tilde{\underline{R}}_Q) + (\tilde{\underline{R}}_A\underline{\underline{P}} + \underline{\underline{G}})\underline{\underline{M}}^{-1}\underline{\underline{P}}^T]\,\underline{v}_s$$

$$= [m_A(\tilde{\underline{R}}_A + \tilde{\underline{r}}_{CA}) + \tilde{\underline{\underline{P}}}\underline{q} + (\tilde{\underline{R}}_A\underline{\underline{P}} + \underline{\underline{G}})M^{-1}\underline{\underline{P}}^T]\,\underline{u}_s + m_o(\tilde{\underline{R}}_D - \tilde{\underline{R}}_Q)\underline{u}_o$$

$$+ [\underline{\underline{I}}_s + \underline{\underline{I}}^*_A + (\tilde{\underline{R}}_A\underline{\underline{P}} + \underline{\underline{G}})\,\underline{\underline{M}}^{-1}(\underline{\underline{G}}^T - \underline{\underline{P}}^T\tilde{\underline{R}}_A)]\,\underline{\omega}_s + \underline{\underline{I}}_o\,\underline{\omega}_o \qquad (47)$$

$$\dot{\underline{q}} = \underline{\underline{M}}^{-1}\underline{\underline{P}}^T(\underline{v}_s - \underline{u}_s) + \underline{\underline{M}}^{-1}[\underline{\underline{G}}^T - \underline{\underline{P}}^T\tilde{\underline{R}}_A](\underline{\Omega}_s - \underline{\omega}_s) \qquad (48)$$

One may obtain from Eqs. (46), (47) and (48) the changes in the state variables which occur during docking. Consideration is now given to the simulation of the motion of the Space Station before and after docking occurs.

SOLUTION TECHNIQUES

Computer programs were developed and used in conjunction with the Harris H-800 minicomputer at Auburn University to simulate the motion of the Space Station. The computer programs consist of three steps, the first of which simulates the motion of the station prior to docking. The second step encompasses the determination of the changes in the kinematical variables due to the docking of an Orbiter with the Space Station. Finally, the third step simulates the motion of the Space Station/Orbiter system after docking has occurred.

In the following sections, the details of the numerical simulation of the Space Station before and after docking are discussed.

Mode Shapes

To describe the deformations of the flexible structure, unconstrained mode shape vectors (eigenvectors) were obtained from a MSC Finite Element program available at Auburn University on the IBM 3033 computer. These mode shape vectors were obtained using the Givens (tridiagonal) method, and were normalized with respect to the mass of the Station.

The truss structure of Fig. 1 was modeled as a structure consisting of "equivalent" beam elements (see Fig. 7). The equivalence was obtained by modeling a section of the truss structure and subjecting it to known forces and torques. With the deformations (both linear and angular) obtained from this model, the stiffness of an equivalent beam was computed using standard beam theory equations.

Using the equivalent beam model for the station, two sets of eigenvectors were obtained. One set contains the eigenvectors for the station without the Orbiter and the other set contains the eigenvectors for the Space Station/Orbiter system. To obtain the eigenvectors for the Space Station/Orbiter system, the Orbiter was modeled as a rigid body attached to the rigid base of the Station.

Numerical Simulation

Equations (28), (29), and (30) represent a set of six plus N (6+N) coupled, second-order differential equations. In the simulation process, these equations are numerically integrated using a fourth-order Runge-Kutta scheme. In order to efficiently utilize the Runge-Kutta scheme, Eqs. (28), (29), and (30) were manipulated to give the following expressions. The expression associated with the generalized coordinates is shown here as

$$[M]\ddot{\underline{q}} + [C]\dot{\underline{q}} + [K]\,\underline{q} = \underline{F} \tag{49}$$

where

$$[M] = -\frac{1}{M_s}\,\underline{\underline{\chi}}^T\underline{\underline{\chi}} + \left[\frac{1}{M_s}\,\underline{\underline{\chi}}^T\underline{\underline{\chi}}\underline{q} + \underline{\underline{\mu}}^T\right]\underline{\underline{I}}^{-1}\left\{-\underline{\underline{\mu}} + \frac{1}{M_s}\,\underline{\underline{\tilde{\chi}}}\underline{q}\underline{\underline{\chi}}\right\}, \tag{50a}$$

$$[C] = -2\zeta[\omega_n]\underline{\underline{M}} \tag{50b}$$

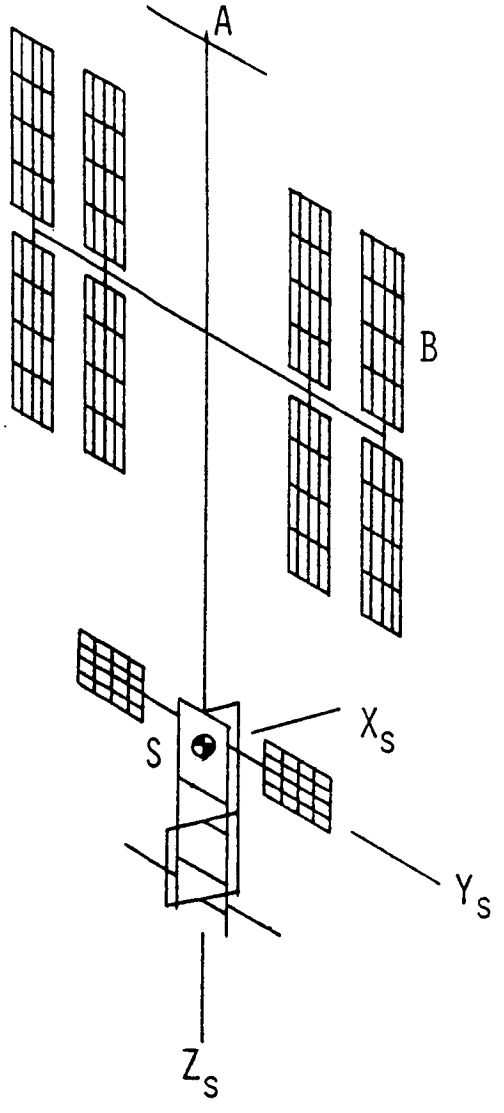

Fig. 7 NASTRAN Equivalent Beam Model.

$$[K] = \frac{1}{M_s}\frac{\mu_o}{R_s^3}\underline{\underline{X}}^T\underline{\underline{X}} - [\omega_n^2]\,\underline{\underline{M}} + \frac{\mu_o}{R_s^3}\underline{\underline{M}}$$

$$+ [\frac{1}{M_s}\underline{\underline{X}}^T\underline{\underline{\tilde{X}}}\underline{q} + \underline{\underline{\mu}}^T]\,\underline{\underline{I}}^{-1}\{\frac{1}{M_s}\frac{\mu_o}{R_s^3}\underline{\underline{\tilde{X}}}\underline{q}\underline{\underline{X}}\}\ , \qquad (50c)$$

and

$$\underline{F} = -\frac{\mu_o}{R_s^3}\underline{\Gamma} - [\frac{1}{M_s}\underline{\underline{X}}^T\underline{\underline{\tilde{X}}}\underline{q} + \underline{\underline{\mu}}^T]\,\underline{\underline{I}}^{-1}\{3\frac{\mu_o}{R_s^5}\underline{\underline{\tilde{C}}}\underline{R}_s\underline{\underline{I}}\underline{\underline{C}}\underline{R}_s\} \qquad (51d)$$

The angular acceleration of the Station is obtained from

$$\dot{\underline{\omega}}_s = \underline{\underline{I}}^{-1}\{3\frac{\mu_o}{R_s^5}\underline{\underline{\tilde{C}}}\underline{R}_s\underline{\underline{I}}\underline{\underline{C}}\underline{R}_s + \frac{1}{M_s}\frac{\mu_o}{R_s^3}\underline{\underline{\tilde{X}}}\underline{q}\underline{\underline{X}}\underline{q}$$

$$+ (-\underline{\mu} + \frac{1}{M_s}\underline{\underline{\tilde{X}}}\underline{q}\underline{\underline{X}})\,\ddot{q}\}\ , \qquad (52)$$

and the linear acceleration of the center of mass of the station is obtained from

$$\ddot{\underline{R}}_s = -\frac{\mu_o}{R_s^3}\underline{R}_s - \frac{1}{M_s}\frac{\mu_o}{R_s^3}\underline{\underline{C}}^T\underline{\underline{X}}\underline{q} + \frac{1}{M_s}\underline{\underline{C}}^T\underline{\underline{\tilde{X}}}\underline{q}\,\dot{\underline{\omega}}_s - \frac{1}{M_s}\underline{\underline{C}}^T\underline{\underline{X}}\underline{q}\ddot{} \qquad (53)$$

In Eqs. (51), (52), and (53),

$$\underline{\underline{X}} = [\underline{m}_1\ \underline{m}_2\ \underline{m}_3\ \cdots\ \underline{m}_N] \qquad (54a)$$

$$\underline{\underline{\mu}} = [\underline{\mu}_1\ \underline{\mu}_2\ \underline{\mu}_3\ \cdots\ \underline{\mu}_N]\ , \qquad (54b)$$

$$\underline{\underline{M}} = \begin{bmatrix} m_{11} & m_{12} & \cdots & m_{1n} \\ m_{21} & m_{22} & \cdots & m_{2n} \\ \vdots & \vdots & & \vdots \\ \dot{m}_{N1} & \dot{m}_{N2} & \cdots & \dot{m}_{NN} \end{bmatrix}\ ,\quad \underline{q} = \begin{bmatrix} q_1 \\ q_2 \\ \vdots \\ \dot{q}_N \end{bmatrix}\ , \qquad (54c,d)$$

$$\underline{\Gamma} = \begin{bmatrix} \gamma_1 \\ \gamma_2 \\ \vdots \\ \gamma_N \end{bmatrix}\ ,\quad \underline{\underline{X}}^T = \begin{bmatrix} \underline{m}_1^T \\ \underline{m}_2^T \\ \vdots \\ \underline{m}_N^T \end{bmatrix}\ ,\quad \underline{\underline{\mu}}^T = \begin{bmatrix} \underline{\mu}_1^T \\ \underline{\mu}_2^T \\ \vdots \\ \underline{\mu}_N^T \end{bmatrix} \qquad (59e,f,g)$$

During the simulation, Eq. (49) is solved for the highest derivative, $\ddot{\underline{q}}$, and then integrated to obtain the time rate of change of the generalized coordinates, $\dot{\underline{q}}$. During each time increment, the calculated values of $\underline{q}$ are substituted into Eq. (51), which is integrated numerically to obtain the angular velocity and angular displacements. A similar process is applied to Eq. (52) to obtain the linear velocity components and linear displacements of the station's mass center.

The process described above is continued until docking occurs. At the instant of "docking," the changes in kinematical variables are obtained by solving Eqs. (46) and (47) simultaneously for the angular velocity, $\underline{\Omega}_s$, and the linear velocity, $\underline{v}_s$, of the station's mass center. These results are then substituted into Eq. (48) to obtain the time rate of change of the generalized coordinates.

Motion after docking is simulated exactly as that before docking, with the exception of accounting for the presence of the Orbiter.

Before any simulation may be accomplished, the initial conditions on $\underline{\omega}_s$, $\underline{R}_s$, q_k, $\dot{q}_k$ and the Orbiter's linear and angular velocity must be given or calculated. This process is considered in the next section.

Initial Conditions

The Space Station's center of mass is assumed to be initially in a 500 km circular orbit inclined at 28.5° (see Fig. 8). Initially, the Station rotates at the mean motion for that orbit. For simplicity, the angle of the ascending node, Ω, was assumed to be zero, and simulation began when the Station occupies the ascending node position. The initial conditions of the generalized coordinate were obtained by assuming a state of dynamic equilibrium for the Space Station. Using these assumptions, the initial conditions on the Space Station state variables were calculated and are shown here in Table 1.

The results discussed in the following sections were obtained using these initial conditions.

RESULTS AND DISCUSSION

An algorithm was developed to numerically integrate the equations of motion of the Space Station and the Space Station/Orbiter system. In this algorithm, a fourth-order Runge-Kutta integration scheme with an integration time increment of 0.01 seconds was used. The motion was simulated over a real time interval of 200 seconds during which docking occurred. A separate algorithm was developed to compute changes that occur in the kinematical variables of the Station due to impulsive docking with the Orbiter. In both algorithms, the structural deformations were calculated using the first eight vibrational modes. A

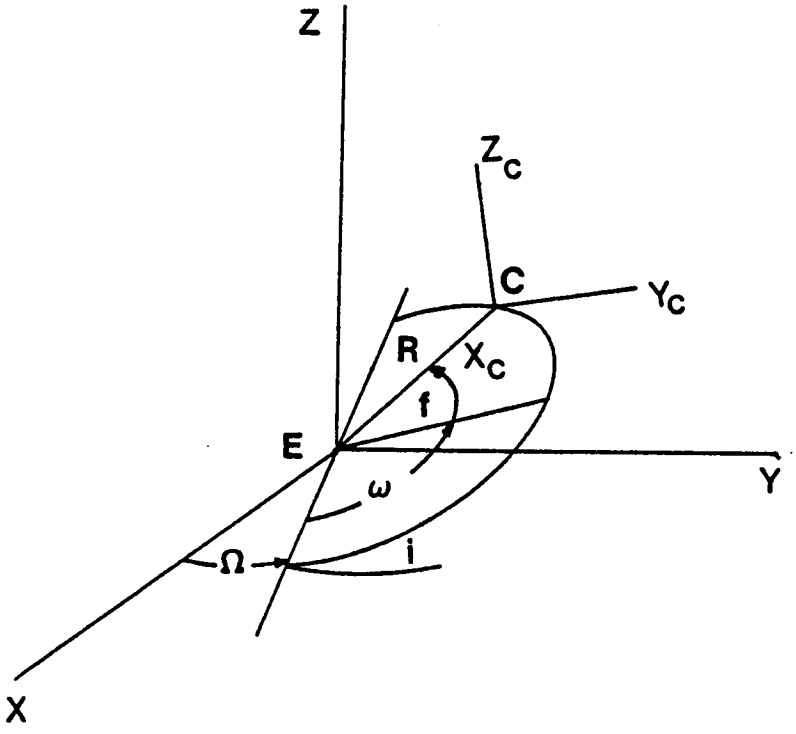

Fig. 8 Orbit Description.

TABLE 1

INITIAL CONDITIONS

Parameter	Initial Value
$\underline{R}_s$ (EXYZ system)	
x-component	6878 km
y-component	0 km
z-component	0 km
$\dot{\underline{R}}_s$ (EXYZ system)	
x-component	0
y-component	7.6127 km/s
z-component	0 km/s
$\underline{\omega}_s$ ($SX_sY_sZ_s$ system)	
x-component	0 rad/s
y-component	0 rad/s
z-component	1.1068×10^{-3} rad/s
q_j, j=1,2,...,N	-0.19623, -0.41874
	0.25247, -0.52811
	0.23838, -0.13866
	0.10141, 0.22680
$\dot{q}_j$, j=1,2,...,N	0, 0, 0,..., 0

third algorithm was developed to compute the mass properties of the Space Station, which are shown in Table 2.

To investigate the effects of docking on motion of the Space Station, three approach orientations of the Orbiter were considered. These are as follows: (1) An approach along the X-axis in the positive X-direction, (2) an approach at 45° to the X-axis in the XY-plane (see Fig. 9), and (3) an approach at 45° to the X-axis in the XZ-plane (see Fig. 9). For each approach orientation, the closing rate of the Orbiter was varied between 0.5 ft/sec and 1.5 ft/sec.

A comparison was made of the changes that occur in the magnitude of the Station's angular velocity when the Station is modeled as a hybrid of flexible and rigid bodies to that of the Station when modeled as a single rigid body. Figures 10 through 14 show this comparison for various approach orientations. It can be observed from these figures that flexibility does affect the angular motion of the Station. The primary effect is due to the time required for the flexible bodies to respond to the impact of the Orbiter with the rigid body to which they are attached. This can be called an "inertia" contribution. Although the cases of Y-axis or Z-axis approach are probably not realistic, it is observed that with either approach the "inertia" contribution of the flexible bodies does not produce significant changes in the angular velocity of the Station's mass center. Thus, for these approaches, the rigid body model yields the larger changes in angular velocity. However, for an approach along the X-axis it is observed that the inertia contribution of the flexible bodies does significantly affect the angular velocity of the Station. Thus, with an X-axis approach, the hybrid model predicts a greater change in angular velocity.

Figure 15 shows the changes in the magnitude of the angular velocity of the hybrid model for approaches (1) along the X-axis, (2) at 45° to the X-axis in the XY-plane, and (3) at 45° to the X-axis in the XZ-plane. It can be observed that the XZ-plane approach produces the smallest changes in the Station's angular velocity.

The simulation results of Figs. 16 through 18 were obtained by numerically integrating the equations of motion of the Station and the Station/Orbiter system. In Eq. (50b), a proportional damping coefficient of 0.01 was assumed. Simulation began when the Station occupied the ascending node position (see Fig. 8); fifty seconds later, docking of the Orbiter occurs. The motion of the Station/Orbiter system after docking is simulated for an additional 150 seconds. The results represented in these figures are the total displacements of the tip of the upper keel (point A) and the center of mass of an upper outboard panel (point B). The deformations of points A and B after docking are observed to be in-phase when the Orbiter approaches along either X-axis or at 45° to the X-axis in the XZ-plane. However, when the the Orbiter's approach is at 45° to the X-axis in the XY-plane, the motion after docking is no longer in-phase. This is probably due to the combined transverse and longitudinal motion of the panels when the approach is in the XY-plane.

TABLE 2

STATION MASS PROPERTIES

WEIGHT	2.6612×10^5 lbs	
MOMENTS AND PRODUCTS OF INERTIA		
IXX	2.0318×10^9	lb-ft^2
IYY	1.8704×10^9	lb-ft^2
IZZ	2.5434×10^8	lb-ft^2
IXY	≈ 0	lb-ft^2
IXZ	7.4644×10^6	lb-ft^2
IYZ	≈ 0	lb-ft^2

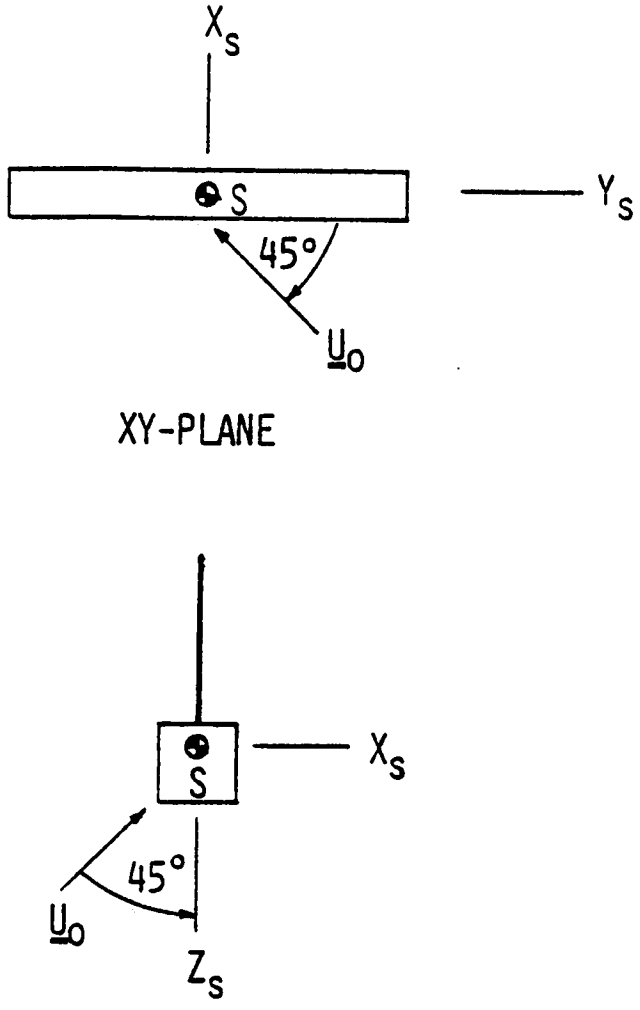

Fig. 9 Approach Orientations for the XY- and XZ-Planes.

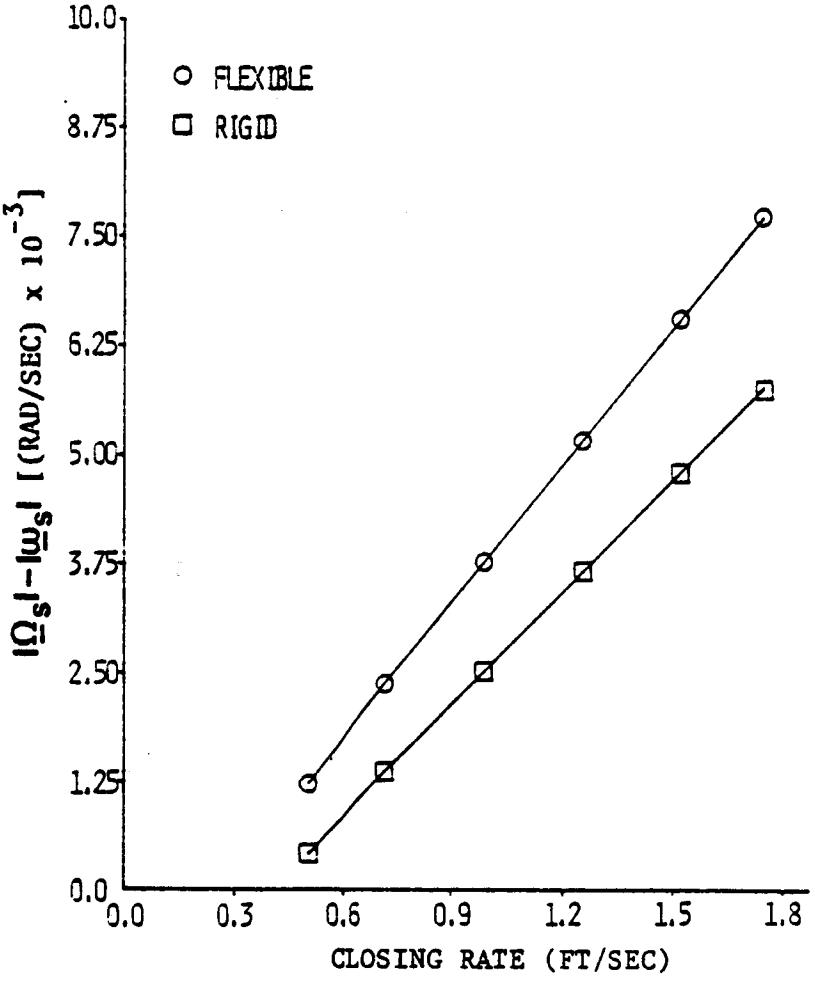

Fig. 10 Change in Angular Velocity Magnitude vs. Closing Rate for an Approach Along the X-axis.

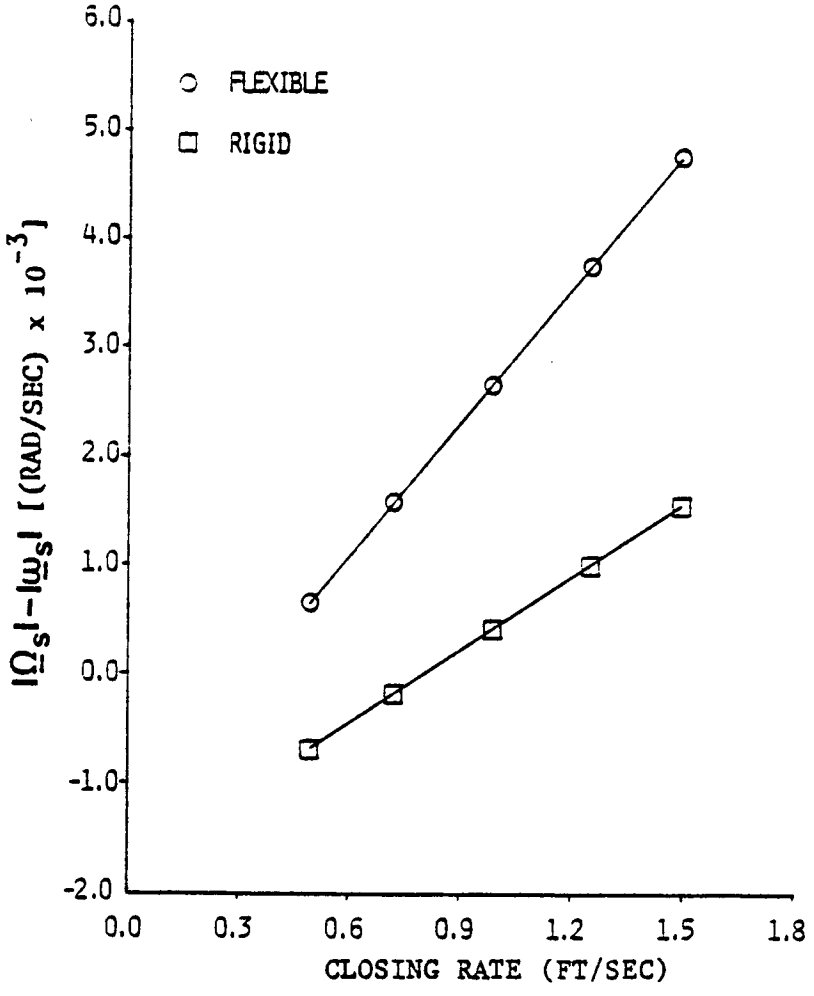

Fig. 11 Change in Angular Velocity Magnitude vs. Closing Rate for an Approach at 45 deg. to the X-axis in the XZ-plane.

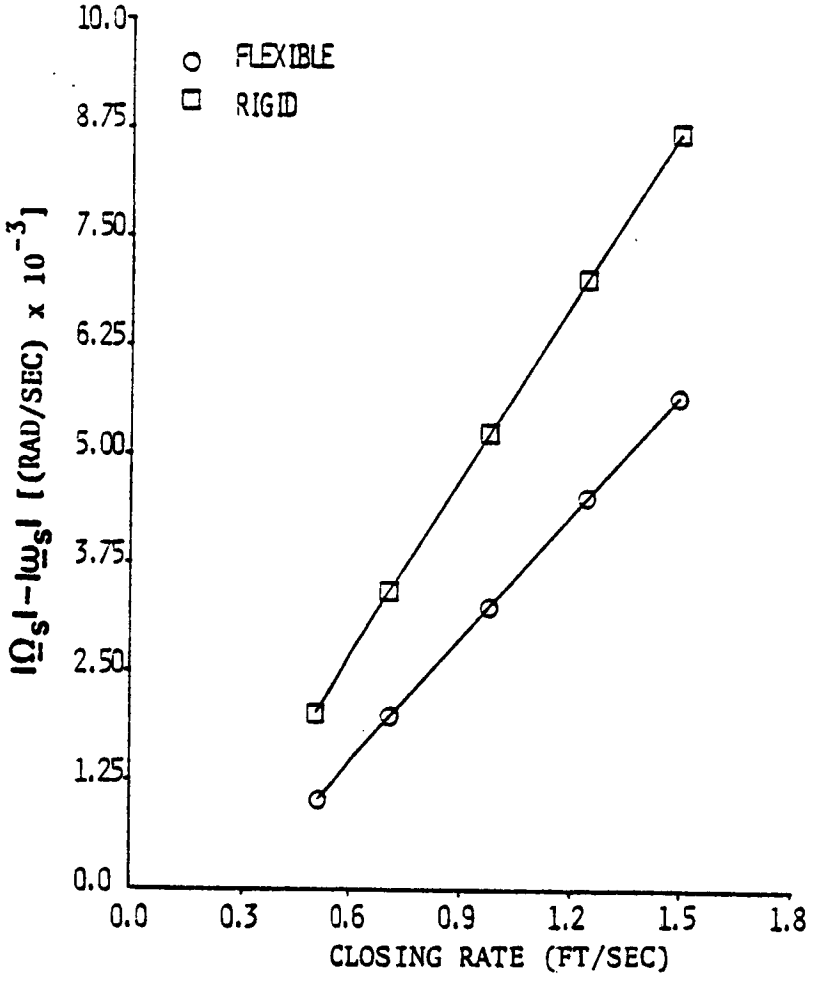

Fig. 12 Change in Angular Velocity Magnitude vs. Closing Rate for an Approach at 45 deg. to the X-axis in the XY-plane.

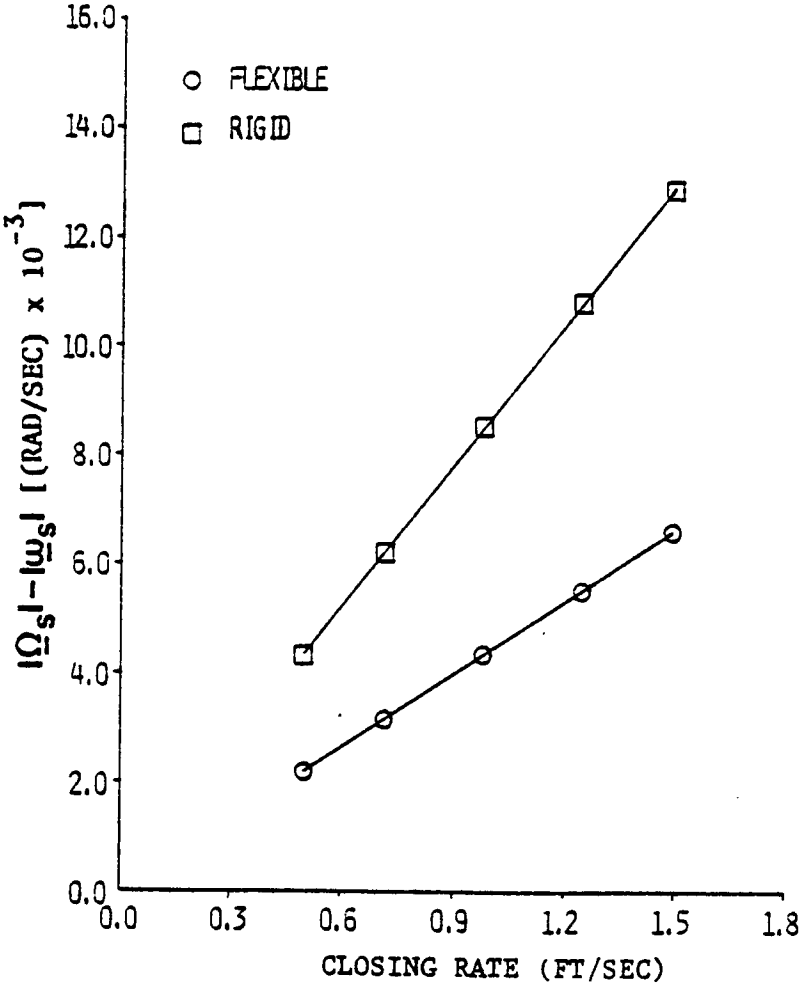

Fig. 13 Change in Angular Velocity Magnitude vs. Closing Rate for an Approach along the Y-axis.

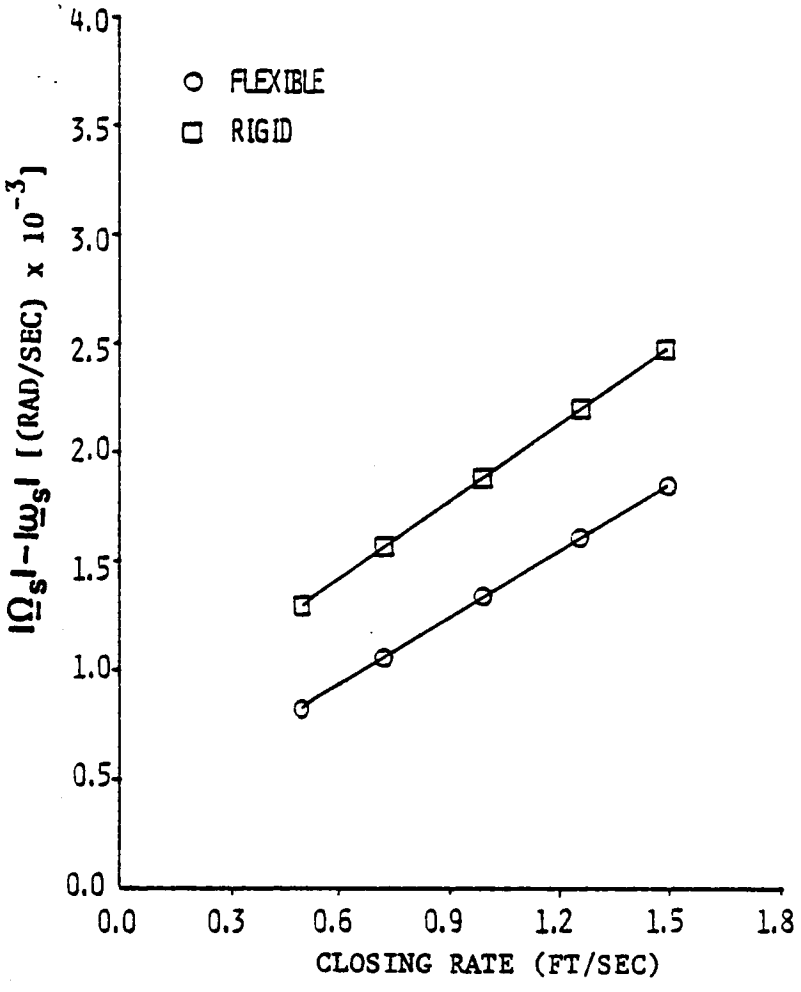

Fig. 14 Change in Angular Velocity Magnitude vs. Closing Rate for an Approach Along the Z-axis.

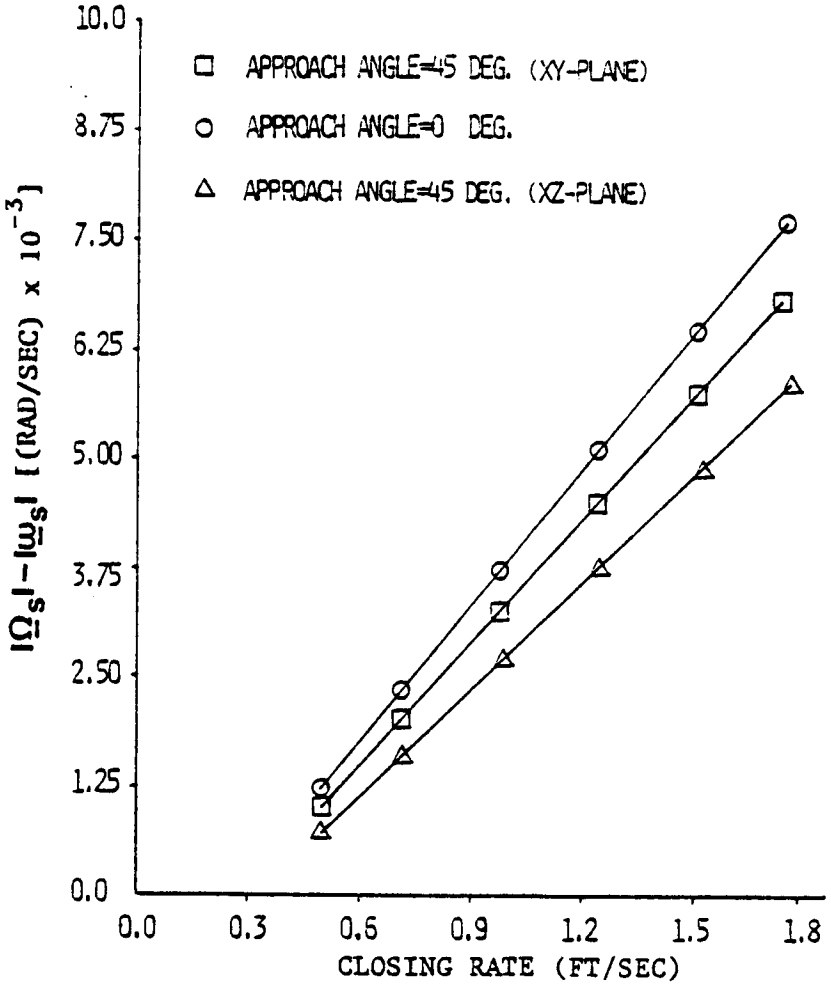

Fig. 15 Comparison of the Change in Angular Velocity Magnitude vs. Closing Rate for the Space Station Modeled as a Hybrid of Flexible and Rigid Bodies.

Figures 16 through 18 also indicate that the maximum deformation of point B is substantially greater than the deformation of point A (approximately twice as large). Figures 19 and 20 show the maximum deformations of points A and B for the various approach orientations and closing rates. An approach along the X-axis produces the greatest maximum deformations, whereas an approach in the XY-plane produces the smallest maximum deformation.

CONCLUSIONS AND RECOMMENDATIONS

The results obtained reveal that flexibility is a significant factor in the dynamics of the docking of an Orbiter with the proposed Space Station. In particular, the changes in the angular velocity of the more rigid part of the Station are greatly affected by flexibility.

Only the first eight modes of vibration were modeled in this analysis. Additional modes of vibrations should be considered in further studies. However, increasing the number of vibrational modes will result in increased computational requirements.

More general results could have been obtained if the Station's payload was considered. In addition, the motion of the crew may have a significant effect on the docking dynamics of the Space Station/Orbiter system.

Finally, a suitable control system must be designed to stabilize the rotational motion of the Station/Orbiter system. Realistically, this can only be done after, or during, a dynamic analysis of a Station model that incorporates payload and crew motion.

ACKNOWLEDGEMENT

This research was supported by the Auburn University Engineering Experiment Station.

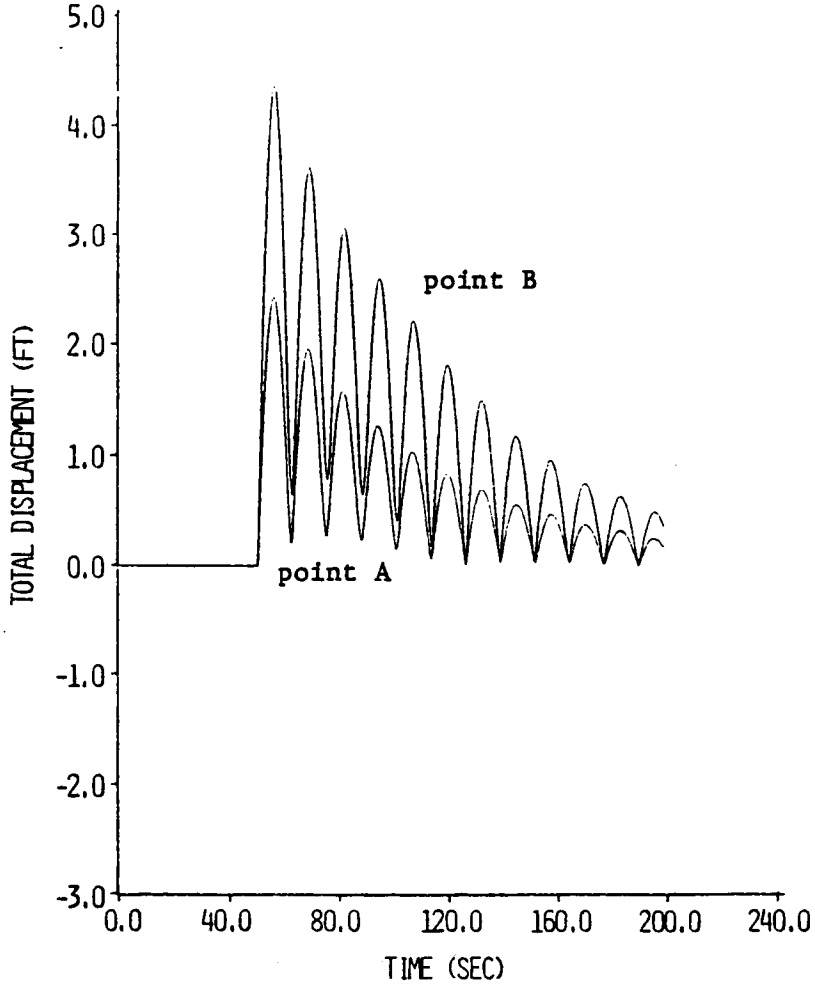

Fig. 16 Displacement Simulation for an Approach Along the X-Axis. (Docking Occurs at T=50 sec.)

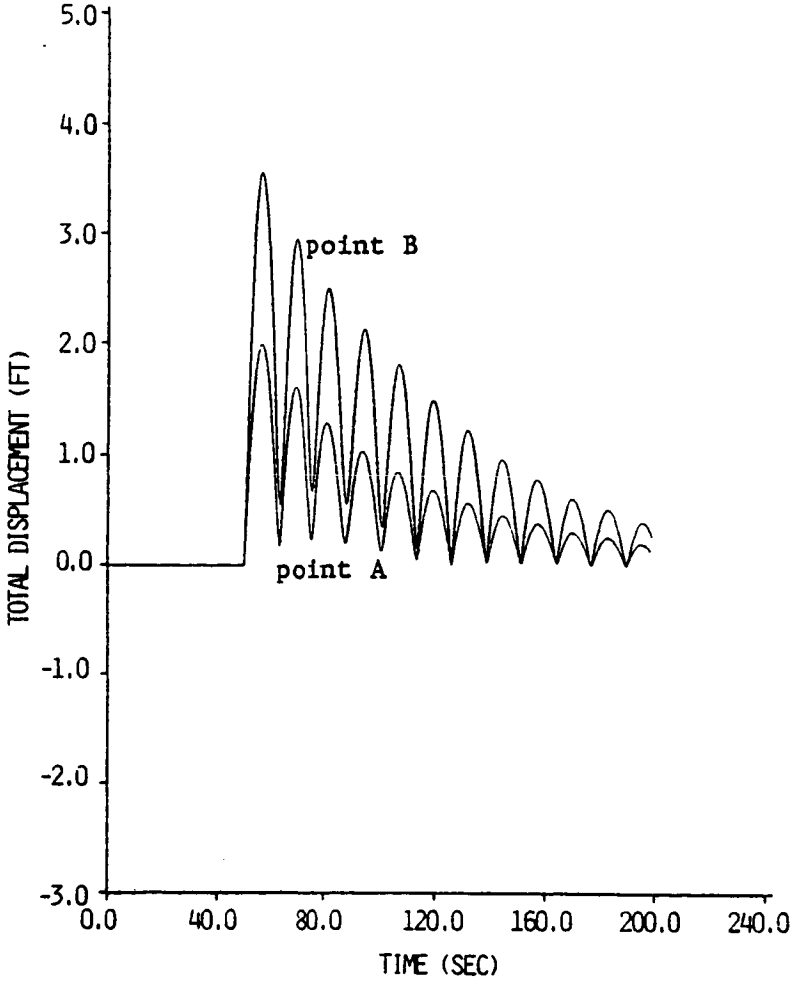

Fig. 17 Displacement Simulation for an Approach at 45° to the X-Axis in the XZ-Plane. (Docking Occurs at T=50 sec.)

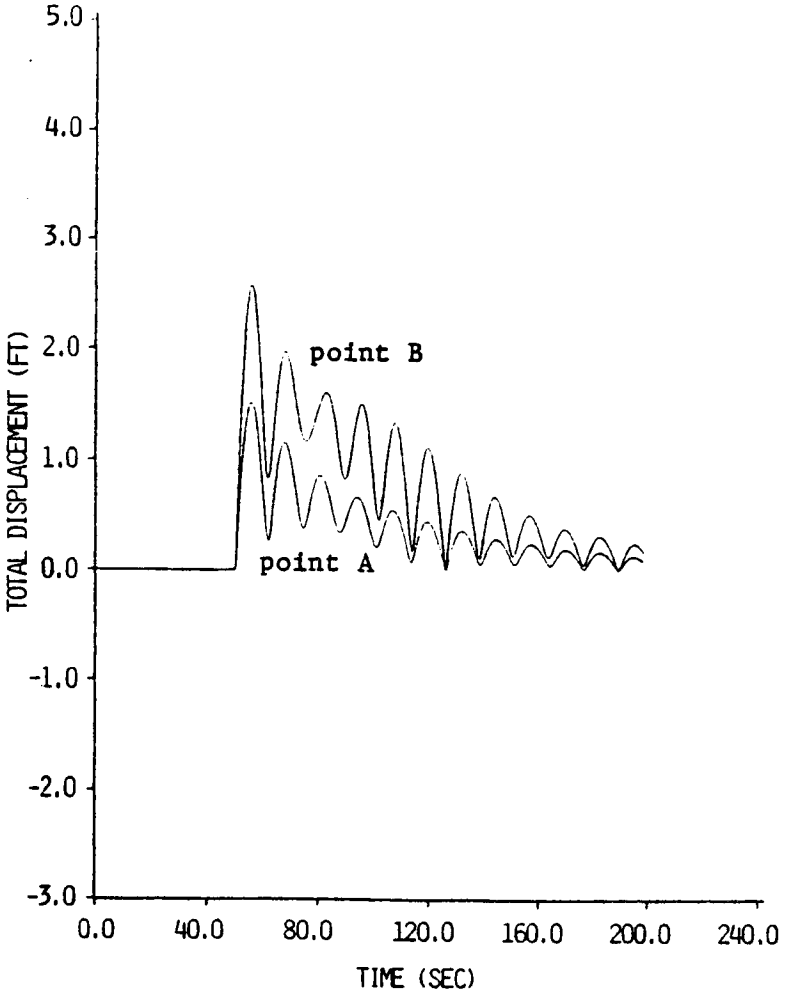

Fig. 18 Displacement Simulation for an Approach at 45^0 to the X-Axis in the XY-Plane. (Docking Occurs at T=50 sec.)

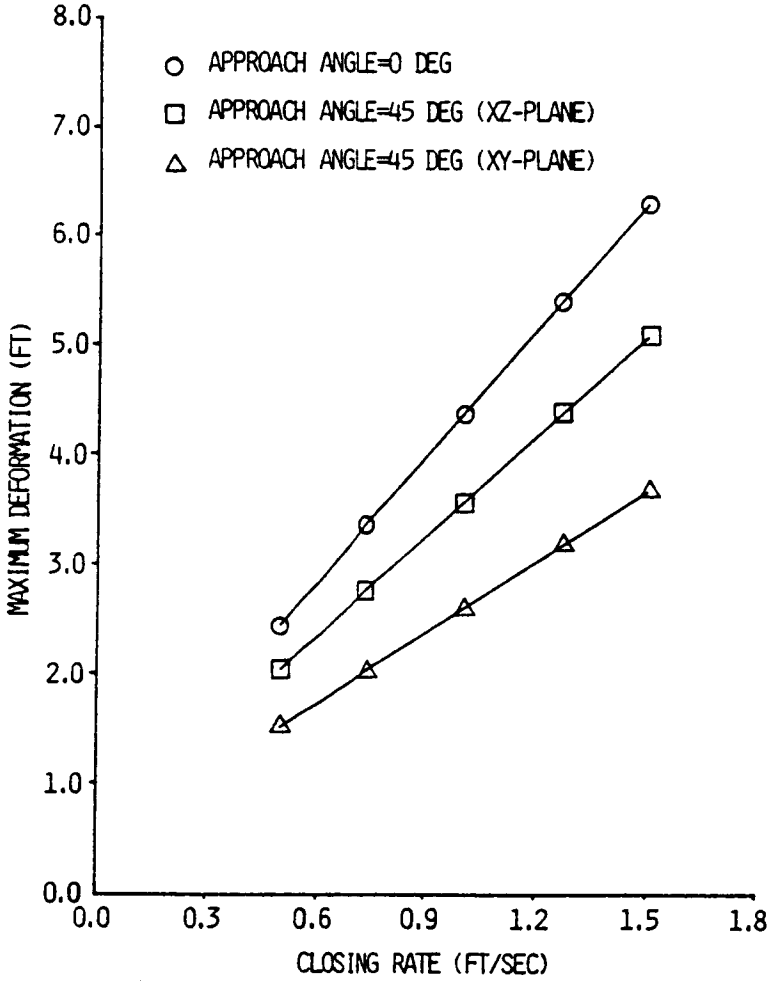

Fig. 19 Maximum Deformation of Point B

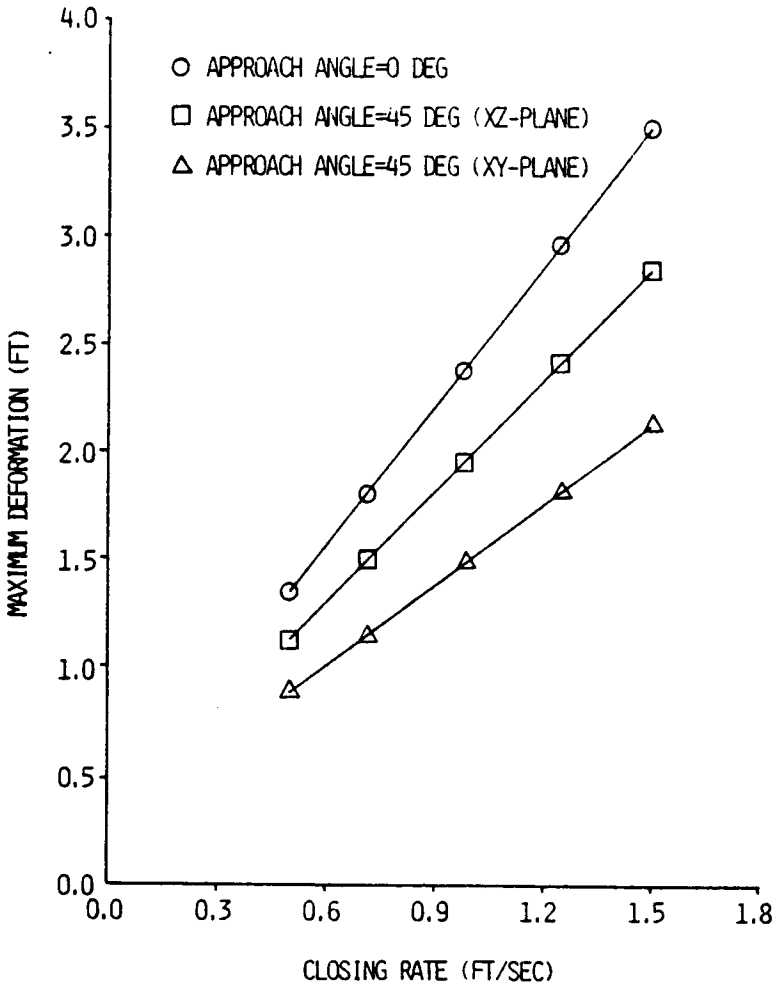

Fig. 20 Maximum Deformation of Point A.

REFERENCES

1. Haggerty, James., Spinoff 1984, National Aeronautics and Space Administration, Office of External Relations, Technology Utilization and Industry Affairs Division, Washington, DC, July 1984, pp. 16-17.

2. JSC-19989, Space Station Reference configuration Description, August 1984.

3. Williams, H. M., and Ward, J. W., "Orbital Docking Dynamics," AIAA Journal, Vol. 1, No. 6, June 1963, pp. 1360-1364.

4. Grubin, C., "Docking Dynamics for Rigid Body Spacecraft," AIAA Journal, Vol. 2, No. 1, January 1964, pp. 5-12.

5. Chiarappa, D., "Rendezvous and Docking," Analysis and Design of Space Vehicle Flight Control System, Vol. VIII, NASA-CR-827, July 1967.

6. Brayton, W. D., "Dynamic Analysis of the Probe and Drogue Docking Mechanism," Journal of Spacecraft and Rockets, Vol. 3, No. 5, May 1966, pp. 700-706.

7. Cochran, J. E., Jr., and Henderson, G. L., Jr, "Docking Dynamics of Spacecraft with Flexible Appendages," Dynamic Analysis of and Synthesis of an Attitude Control System for a Spacecraft to Rendezvous with Comets and Asteroids, Vol. IV, Final Report, contract NAS8-28110, Auburn University, Auburn, Alabama, July 31, 1973.

8. Kane, T. R., and Levinson, D. A., "Simulation of Large Motions of Nonuniform Beams in Orbit, Part II - The Unrestrained Beam," Journal of the Astronautical Sciences, Vol. XXIX, No. 3, July-September 1981, pp. 245-275.

9. Levinson, D. A., and Kane, T. R., "Simulaiton of Large Motions of Nonuniform Beams in Orbit, Part I - The Cantilever Beam," Journal of the Astronautical Sciences, Vol. XXIX, No. 3, July-September 1981, pp. 213-244.

10. Levinson, D. A., and Kane, T. R., "Docking of a Spacecraft with an Unrestrained Orbiting Structure," Journal of Astronautical Sciences, Vol. XXXI, No. 1, January-March 1983, pp. 23-48.

11. Hablani, Hari B., "Constrained and Unconstrained Modes: Some Modeling Aspects of Flexible Spacecraft," Journal of Guidance, Control, and Dynamics, Vol. 5, No. 2, March-April 1982.

12. Likins, P. W., "Analytical Dynamics and Nonrigid Spacecraft Simulation," Technical Report 32-1593, Jet Propulsion Laboratory, Pasadena, California, July 15, 1974.

13. Hughes, P. C., and Skelton, R. E., "Modal Truncation for Flexible Spacecraft," Journal of Guidance and Control, Vol. 4, No. 3, May-June 1981.

14. Ho, J. Y. L., and Herber, D. R., "Development of Dynamics and Control Simulation of Large Flexible space systems," Journal of Guidance, Control, and Dynamics, Vol. 8, No. 3, May-June 1985.

15. Kane, T. R., and Levinson, D. A., "Formulation of Equations of Motion for Complex Spacecraft," Journal of Guidance and Control, Vol. 3, No. 2, March-April 1980.

16. Schaeffer, Harry G., MSC/NASTRAN Primer: Static and Normal Modes Analysis, Schaeffer Analysis, Inc., 1982.

17. Kane, T. R., Dynamics, Second Edition, Stanford University, 1972.

18. Kaplan, M. H., Modern Spacecraft Dynamics and Control, John Wiley & Sons, 1976.